

VESSEL TREE SEGMENTATION VIA FRONT PROPAGATION AND DYNAMIC ANISOTROPIC RIEMANNIAN METRIC

Da Chen and Laurent D. Cohen

CEREMADE, UMR 7534, CNRS, Université Paris Dauphine PSL*, 75775 Paris Cedex 16, France

ABSTRACT

In this paper, we present a blood vessel segmentation method by front propagation and anisotropic Riemannian metric. The front is defined as the level set of the geodesic distance to a set of given initial source points, with respect to a dynamic anisotropic Riemannian metric. The boundaries of the vessels can be represented by the level set at the given distance threshold. The anisotropic Riemannian metric can be defined using a prior estimate of the vessel orientations and the local intensity difference values, where the vessel orientations are detected by the oriented flux filter. Experimental results demonstrate the proposed vessel detection method indeed outperforms the traditional vesselness based detection method.

Index Terms— Vessel tree segmentation, level set, Fast Marching method, dynamic anisotropic Riemannian metric.

1. INTRODUCTION

Vessel tree extraction is an essential task in medical imaging and computer-assisted therapy applications. Various vasculature structure segmentation methods, such as vessel enhancement methods and deformable models have been studied during the passed three decades [1].

Multi-scale vessel enhancement methods like Hessian based vessel enhancement filter [2, 3, 4, 5], convert the vessel intensity into the vesselness value, where each pixel value indicates the probability of this pixel belonging to a vessel. Then the binary segmented image can be obtained by thresholding the vesselness image. This class of models sometimes suffer from the scale overfitting problem when treating two vessels that are closed to each other.

Flux based active contours have been widely applied to tubular structure segmentation since the pioneer work presented in [6], in which the flux magnitude field of the image gradient vector is taken as the dominating external force to drive the active contours (2D) or active surfaces (3D) to sketch the tubular structure boundaries. To solve the expensive computation of the flux, Law *et al.* proposed a fast flux computation method [7] and its improved method: optimally oriented flux filter [3] which be adapted to active contours models [8]. However, those deformable models are based on the level set evolution scheme, where the curve or surface is

defined as a zero level set, suffering from high computational complexity.

Fast Marching based front propagation method was developed to overcome the computational complexity of classical level set numerical scheme by Malladi *et al.* [9]. This requires the speed to be positive everywhere, making the front propagation based segmentation [9, 10] to suffer from leakage, i.e., some parts of the front need more time to reach the boundaries, and by that time, other parts of the front leak across the boundary. The authors in [10] proposed a curve length based front propagation method which can classify the front points into *head* and *tail*. Then the tail points are frozen to prevent leakages. The main drawback of those front propagation methods is they are only based on *isotropic* metric.

In this work, we proposed an improved front propagation method for blood vessel segmentation, based on a *dynamic anisotropic* Riemannian metric calculated from the current front and local intensities. The orientation of each pixel are computed using the optimally oriented flux filter [3]. The motivation of this work is that vesselness based segmentation methods like [3] may suffer from the scale overfitting problems and are difficult to combine with manual interventions. Additionally, for isotropic Fast Marching front propagation, leakage problem often occurs. Instead, our method can easily take into account the user defined initial points and will avoid leaking problem thanks to the dynamic Riemannian metric field and the orientation enhancement.

2. BACKGROUND

2.1. Front Propagation Segmentation

We consider the isotropic Eikonal equation:

$$\mathcal{P}(\mathbf{x})\|\nabla\mathcal{U}(\mathbf{x})\| = 1, \quad (1)$$

where \mathcal{U} is the minimal action map or minimal arrival time with speed function $\mathcal{P} : \Omega \rightarrow \mathbb{R}^+$ with $\Omega \subset \mathbb{R}^2$ being the image domain. This Eikonal equation was first adapted by [9] for surface segmentation since it shares some of the evolutionary property of level set based method but with much cheaper computational time.

Given a set of initial source points, the behaviour of the front propagation is like the curve evolution driven by a bal-

lon force [11]. Generally, the speed function \mathcal{P} should be large inside the flat region in order for the front to propagate very fast. In contrast, at the vicinity of boundaries, \mathcal{P} should become small and the front propagation will be slow in this region, thus stopping the front to leak out the vessels. \mathcal{P} might depend on the image gradient or vesselness values.

Numerically, the Eikonal equation (1) can be solved by the Fast Marching algorithm [12]. The gradient $\nabla\mathcal{U}$ is approximated by a first order upwind scheme, satisfied for the isotropic metric \mathcal{P} . In this paper, we focus on the anisotropic Riemannian metric which cannot be solved by such Fast Marching method. Instead, we utilize the anisotropic Fast Marching algorithm proposed in [13] which is very stable even for large anisotropy ratio.

2.2. Optimally Oriented Flux Filter

The optimally oriented flux filter [3] was designed to compute the vesselness map at the optimal scale and get the orientations of each point inside the vessels. For a given two-dimensional image I , flux f is defined as the summation of the image gradient projected along the orientation vector \vec{p} , flowing out from a circle centred at point \mathbf{x} with radius r :

$$f(\mathbf{x}; r, \vec{p}) = \int_{\partial\mathcal{C}_r} \left(\nabla(G_\sigma * I)(\mathbf{x} + r\vec{n}) \cdot \vec{p} \right) (\vec{p} \cdot \vec{n}) ds. \quad (2)$$

Where G_σ is a Gaussian with variance σ , which is used to smooth I and the outward unit normal vector along $\partial\mathcal{C}_r$ is represented by \vec{n} . By the divergence theory [3], the oriented flux f can be expressed as $f(\mathbf{x}; r, \vec{p}) = \langle \vec{p}, \mathcal{Q}(\mathbf{x}, r) \cdot \vec{p} \rangle$, where \mathcal{Q} is a symmetric matrix defined by the oriented flux filter \mathbf{F}_r :

$$\mathcal{Q}(\mathbf{x}, r) = \left(\left(\frac{1}{r} \mathbf{F}_r \right) * I \right) (\mathbf{x}, r). \quad (3)$$

See [3] for more details about \mathbf{F}_r . For each point (\mathbf{x}, r) , \mathcal{Q} can be decomposed using eigenvectors as: $\mathcal{Q}(\mathbf{x}, r) = \sum_{i=1}^2 \lambda_i(\mathbf{x}, r) \vec{u}_i(\mathbf{x}, r) \otimes \vec{u}_i(\mathbf{x}, r)$.

Supposing the intensity values inside the vessels are higher than outside and $\lambda_1(\cdot) \leq \lambda_2(\cdot)$, one has: $\forall \mathbf{x}$ inside vessels, $\lambda_1(\mathbf{x}, \cdot) \ll \lambda_2(\mathbf{x}, \cdot) \approx 0$, which means λ_1 is negative and has a large absolute value. Then the vesselness map $\mathcal{I} : \Omega \rightarrow \mathbb{R}$ is defined as:

$$\mathcal{I}(\mathbf{x}) = |\lambda_1(\mathbf{x}, r^*(\mathbf{x}))|, \quad r^*(\mathbf{x}) = \arg \max_r |\lambda_1(\mathbf{x}, r)|.$$

Similarly, we define the vessel orientation field \vec{V} :

$$\vec{V}(\mathbf{x}) = \vec{u}_2(\mathbf{x}, r^*(\mathbf{x})). \quad (4)$$

We will use this orientation vector field \vec{V} to construct our Riemannian metric in the following section.

3. DYNAMIC RIEMANNIAN METRIC BASED FRONT PROPAGATION

3.1. Front Propagation with Anisotropic Metric

In this section, we consider the anisotropic Eikonal equation with Riemannian metric. For a symmetric positive tensor field \mathcal{M} , the anisotropic Eikonal equation is

$$\|\nabla\mathcal{U}(\mathbf{x})\|_{\mathcal{M}^{-1}(\mathbf{x})} = 1. \quad (5)$$

The anisotropic Fast Marching algorithm [13] can be used as the numerical solver of distance map \mathcal{U} , by finding the solution, at each update step, of the fixed point problem:

$$\mathcal{U}(\mathbf{x}) = \min_{\mathbf{y} \in \partial S(\mathbf{x})} \left\{ \mathcal{L}(\mathbf{x}, \mathbf{y} - \mathbf{x}) + \mathcal{I}_{S(\mathbf{x})} \mathcal{U}(\mathbf{y}) \right\}, \quad (6)$$

$$\mathcal{L}(\mathbf{x}, \vec{v}) = \sqrt{\langle \vec{v}, \mathcal{M}(\mathbf{x}) \vec{v} \rangle},$$

where $\mathcal{I}_{S(\mathbf{x})}$ is a piecewise linear interpolation operator on a mesh $S(\mathbf{x})$. The local mesh or stencil S can be adaptively constructed according to the given Riemannian metric \mathcal{M} by the tool of Lattice Basis Reduction, as introduced in [13], leading to breakthrough improvements in terms of computational time and accuracy when dealing with metrics having strong anisotropy ratio.

As initialization, the Fast Marching algorithm tags all the discretization grid points of Ω into three labels: *Alive*, points have been computed and frozen; *Trial*, points have been updated at least once but not frozen; and *Far*, points have not been estimated yet. The Fast Marching *front* consists of all the *Trial* points. At each update iteration, the *Trial* point \mathbf{x} , minimizing \mathcal{U} , will be selected and tagged as *Alive* and all the neighbour points $\mathbf{y}_\mathbf{x} \in \{\mathbf{y} \in \Omega; \mathbf{x} \in S(\mathbf{y})\}$ will be updated by solving (6). For convenience, we say that point \mathbf{x} is **base-point** of all its neighbour points $\mathbf{y}_\mathbf{x}$ in this update step.

3.2. Dynamic Riemannian Metric Construction

Traditional anisotropic Eikonal equation uses static metric field independent of the Fast Marching front. For blood vessels segmentation application, one has to deal with the problem of intensities inhomogeneities which is not suitable for the static metric, thus we propose to take into account the front location to calculate *dynamic* metric field.

Assuming that vessels are brighter than background and letting $\mathcal{A} \subseteq \Omega$ be a collection of all points tagged as *Alive*, we define a local mean intensity function $\mathcal{K} : \Omega \rightarrow \mathbb{R}^+$ and a local intensity difference map $\mathcal{J} : \Omega \rightarrow \mathbb{R}^+$:

$$\mathcal{K}(\mathbf{x}) := \sum_{\mathbf{y} \in \mathcal{A} \cap B_r(\mathbf{x})} I(\mathbf{y}) / \# \left\{ \mathcal{A} \cap B_r(\mathbf{x}) \right\}, \quad (7)$$

$$\mathcal{J}(\mathbf{x}) := \exp(\alpha |\min\{I(\mathbf{x}) - \mathcal{K}(\mathbf{x}), 0\}|), \quad \mathbf{x} \in \Omega. \quad (8)$$

Where α is a positive constant. $B_r(\mathbf{x})$ is a ball with radius r defined as $\{\mathbf{p}; \|\mathbf{x} - \mathbf{p}\| \leq r\}$. $\# \{ \mathcal{A} \cap B_r(\mathbf{x}) \}$ is the number

Algorithm 1 *FrontPropagationwithDynamicMetric*

Input: Tensor field \mathcal{M}_c , initial point set \mathcal{W} and stencil S .

Output: Minimal action map \mathcal{U} .

Initialization:

- For each point $\mathbf{x} \in \Omega$, set $\mathcal{U}(\mathbf{x}) = +\infty$ and $\mathcal{D}(\mathbf{x}) = \text{Far}$.
- For each point $\mathbf{x} \in \mathcal{W}$, set $\mathcal{U}(\mathbf{x}) = 0$ and $\mathcal{D}(\mathbf{x}) = \text{Trial}$.

While(stopping criterion is not reached)

- 1: Find \mathbf{x}_{\min} , the *Trial* point which minimizes \mathcal{U} .
 - 2: $\mathcal{A} \leftarrow \mathbf{x}_{\min}$ and $\mathcal{D}(\mathbf{x}_{\min}) \leftarrow \text{Alive}$.
 - 3: Compute $\mathcal{K}(\mathbf{x}_{\min})$ using (7).
 - 4: **for** All \mathbf{y} such that $\mathbf{x}_{\min} \in S(\mathbf{y})$ and $\mathcal{D}(\mathbf{y}) \neq \text{Alive}$ **do**
 - 5: Update $\mathcal{J}(\mathbf{y})$ using (10).
 - 6: Construct the tensor field \mathcal{M}_d using (11).
 - 7: Compute $\mathcal{U}_{\text{new}}(\mathbf{y})$ using (6).
 - 8: **if** $\mathcal{U}_{\text{new}}(\mathbf{y}) < \mathcal{U}(\mathbf{y})$ **then**
 - 9: $\mathcal{U}(\mathbf{y}) \leftarrow \mathcal{U}_{\text{new}}(\mathbf{y})$ and $\mathcal{D}(\mathbf{y}) \leftarrow \text{Trial}$.
 - 10: **end if**
 - 11: **end for**
-

of points contained in the set $\mathcal{A} \cap B_r(\mathbf{x})$. \mathcal{K} is computed only inside a local region such that the proposed front propagation method is robust when dealing with intensity inhomogenities and noise. By assuming that vessels have higher gray levels, we consider that if a pixel \mathbf{x} has higher intensity than the average intensity value of its vicinity points defined by $B_r(\mathbf{x}) \cap \mathcal{A}$, \mathbf{x} is likely to be located inside a vessel. Therefore we use $|\min\{I(\mathbf{x}) - \mathcal{K}(\mathbf{x}), 0\}|$ to calculate $\mathcal{J}(\mathbf{x})$ in (8) instead of using $|I(\mathbf{x}) - \mathcal{K}(\mathbf{x})|$.

Numerically, function \mathcal{J} will be updated in each update iteration of the Fast Marching algorithm. To reduce the computational complexity, we use the following approximation:

$$\mathcal{K}(\mathbf{x}) \approx \mathcal{K}(\mathbf{z}), \quad (9)$$

where \mathbf{z} is a *base-point* of \mathbf{x} . Then \mathcal{J} can be approximated by

$$\mathcal{J}(\mathbf{x}) \approx \exp(\alpha |\min\{I(\mathbf{x}) - \mathcal{K}(\mathbf{z}), 0\}|). \quad (10)$$

With this approximation, \mathcal{J} only requires to be updated N times where N is the total number of grid points in I .

The dynamic tensor field (anisotropic Riemannian metric) \mathcal{M}_d can be constructed by combination of \mathcal{J} as:

$$\mathcal{M}_d(\mathbf{x}) = \mathcal{J}(\mathbf{x}) \times \mathcal{M}_c(\mathbf{x}), \quad (11)$$

$$\mathcal{M}_c(\mathbf{x}) = \vec{V} \otimes \vec{V}(\mathbf{x}) + \mu \times \vec{V}^\perp \otimes \vec{V}^\perp(\mathbf{x}). \quad (12)$$

where \vec{V}^\perp is the vector field orthogonal to \vec{V} and \vec{V} is the vessel orientation vector field defined in (4). μ is the anisotropic ratio. One can see that \mathcal{M}_c is a non-changed tensor field during the Fast Marching front propagation. In contrast, \mathcal{M}_d will be updated in each Fast Marching update iteration due to the computation of \mathcal{J} . In Algorithm 1, we present the details of our algorithm. \mathcal{A} , \mathcal{K} , and \mathcal{J} are updated in lines 2, 3 and 5 respectively. The *stopping criterion* is a threshold computed

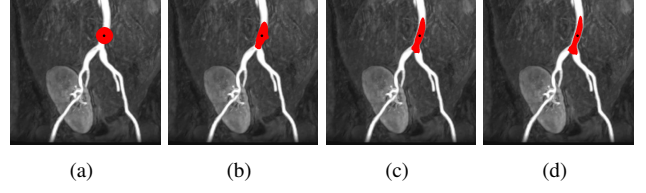


Fig. 1. Front propagation based on \mathcal{M}_c in (12) for different ratio μ .

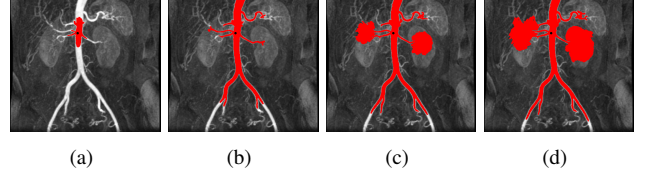


Fig. 2. Front propagation using isotropic Fast Marching method and \mathcal{J} .

by making sure that $T\%$ of pixels having the lowest minimal action map \mathcal{U} , among all pixels, have been chosen. For Fast Marching algorithm, this *stopping criterion* is equivalent to find $N * T\%$ points tagged as *Alive*, where N is the total number of image pixels.

4. EXPERIMENTS

We first show the advantage of using anisotropic Riemannian metric rather than isotropic metric. Fig. 1 shows four front propagation results with the same number of points tagged as *Alive*. The anisotropic ratio values for Fig. 1(a)-(d) are 1, 10, 30, and 50 respectively. It can be seen that a large anisotropic ratio could make the front propagate along the vessel structure as far as possible before the front leaks out of the vessels. In the following experiments, we set the anisotropic ratio value to be 30 for the proposed method.

In Fig. 2, we show the segmentation results using $1/\mathcal{J}$ as the speed for the *isotropic* front propagation. At the beginning of the front propagation in Fig. 2(a) and (b), no leakage happens. However, as the front goes further along interior region of the vessel tree, it leaks from some weak vessels. This is why we utilize the anisotropic front propagation method.

In Fig. 3, we show the segmentation results from three segmentation methods: the second column shows the results by thresholding the vesselness map \mathcal{I} in (4); the third column is obtained from a front propagation based method, in which we set the metric as

$$\mathcal{M}(\mathbf{x}) = \exp(\beta \mathcal{I}(\mathbf{x})) (\vec{V} \otimes \vec{V}(\mathbf{x}) + \mu \vec{V}^\perp \otimes \vec{V}^\perp(\mathbf{x})),$$

with $\beta < 0$. For fair comparison, we use the same Fast Marching algorithm [13] with the proposed method to compute the minimal action map. Black points in the third and last columns are the initial source points. The last column gives the results by the proposed method. All the three methods require thresholding to get the final segmentation results.

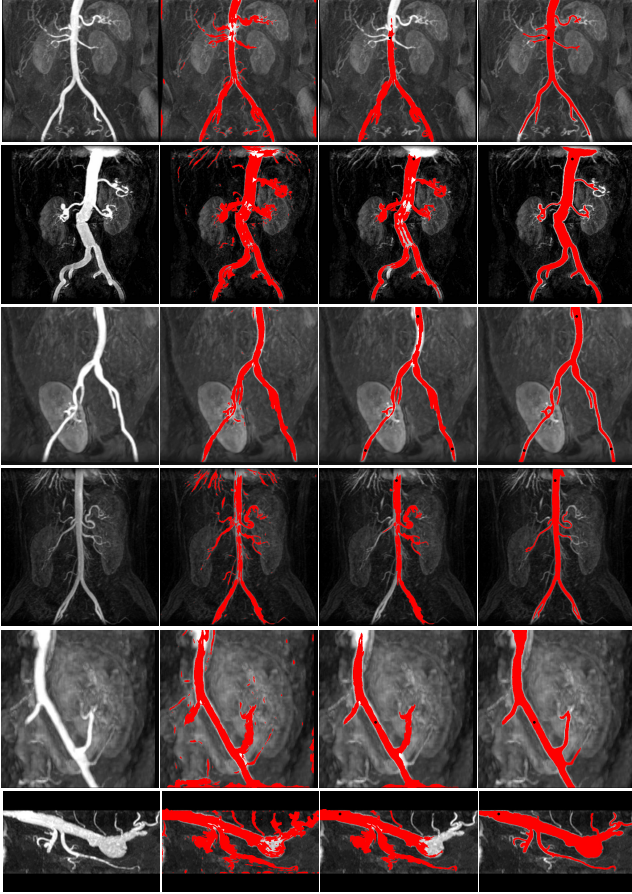


Fig. 3. Vessel tree segmentation results from different methods. (see text)

One can see that the vesselness based results have many holes and scale overfitting. The vesselness-based front propagation method also suffers from the similar problems since the distance maps are heavily affected by the vesselness. In contrast, the proposed method can avoid the mentioned problems. In this experiment, we choose the same T for the front propagation methods (third and last columns) but a little bigger T_1 to threshold the \mathcal{I} in the second column.

5. CONCLUSION

In this paper, we propose a new front propagation method for vessel segmentation with the dynamic anisotropic Riemannian metric and anisotropic Fast Marching. We use the local intensity coherence to penalize the tensor field constructed by the vessel anisotropy to make the front propagation robust to vessel intensity inhomogeneities and noise. Experiments show that our model indeed obtain expected results.

Acknowledgement

This work was partially supported by ANR grant NS-LBR, ANR-13-JS01-0003-01.

6. REFERENCES

- [1] C. Kirbas and F. Quek, "A review of vessel extraction techniques and algorithms," *ACM Computing Surveys*, vol. 36, no. 2, pp. 81–121, 2004.
- [2] A. F. Frangi, W. J. Niessen, Koen L. Vincken, and Max A. Viergever, "Multiscale vessel enhancement filtering," in *MICCAI*, 1998, pp. 407–433.
- [3] M. Law and A. Chung, "Three Dimensional Curvilinear Structure Detection Using Optimally Oriented Flux," in *ECCV*, 2008, pp. 368–382.
- [4] J. Hannink, R. Duits, and E. Bekkers, "Crossing-preserving multi-scale vesselness," in *MICCAI*, 2014, pp. 603–610.
- [5] C. Xiao, M. Staring, Y. Wang, D. P. Shamonin, and B. C. Stoel, "Multiscale bi-Gaussian filter for adjacent curvilinear structures detection with application to vasculature images," *TIP*, vol. 22, no. 1, pp. 174–188, 2013.
- [6] A. Vasilevskiy and K. Siddiqi, "Flux maximizing geometric flows," *PAMI*, vol. 24, no. 12, pp. 1565–1578, 2002.
- [7] M. Law and A. Chung, "Efficient implementation for spherical flux computation and its application to vascular segmentation," *TIP*, vol. 18, no. 3, pp. 596–612, 2009.
- [8] M. Law and A. Chung, "An Oriented Flux Symmetry based Active Contour Model for Three Dimensional Vessel Segmentation," in *ECCV*, 2010, pp. 720–734.
- [9] R. Malladi and J. A. Sethian, "A real-time algorithm for medical shape recovery," in *ICCV*, 1998, pp. 304–310.
- [10] L. Cohen and T. Deschamps, "Segmentation of 3D tubular objects with adaptive front propagation and minimal tree extraction for 3D medical imaging," *Comput. Method Biomec.*, vol. 10, no. 4, pp. 289–305, 2007.
- [11] L. D. Cohen, "On active contour models and balloons," *CVGIP: Image understanding*, vol. 53, no. 2, pp. 211–218, 1991.
- [12] J. A. Sethian, "Fast marching methods," *SIAM Review*, vol. 41, no. 2, pp. 199–235, 1999.
- [13] Jean-Marie Mirebeau, "Anisotropic Fast-marching on Cartesian Grids Using Lattice Basis Reduction," *SIAM J. Numer. Anal.*, vol. 52, no. 4, pp. 1573–1599, 2014.